

1
2
3
4
5
6
7
8
9
10
11
12
13
14
15
16
17
18
19
20
21

**Drug release from magnesium aluminium silicate-polyethylene oxide
(PEO) nanocomposite matrices: An investigation using the USP III
apparatus**

Kofi Asare-Addo^{a*}, Ana-Maria Totea^a, Ali Nokhodchi^{b*}

^aUniversity of Huddersfield, Department of Pharmacy, Queensgate, Huddersfield, HD1 3DH

^bPharmaceutics Research Laboratory, School of Life Sciences, University of Sussex,
Brighton, BN1 9QJ, UK

*Corresponding author: Dr Kofi Asare-Addo

Email: k.asare-addo@hud.ac.uk

[Tel: 01484472360](tel:01484472360)

Corresponding author: Professor Ali Nokhodchi

Email: A.Nokhodchi@sussex.ac.uk

Submission: EJPS

22 **Highlights**

23 ITC results show binding between DILT and PEO was enthalpy and entropy driven

24 Binding between veegum and DILT in the presence of PEO shown to be enthalpy driven and
25 entropically unfavourable

26 ITC results successfully explain drug release from veegum-PEO matrices

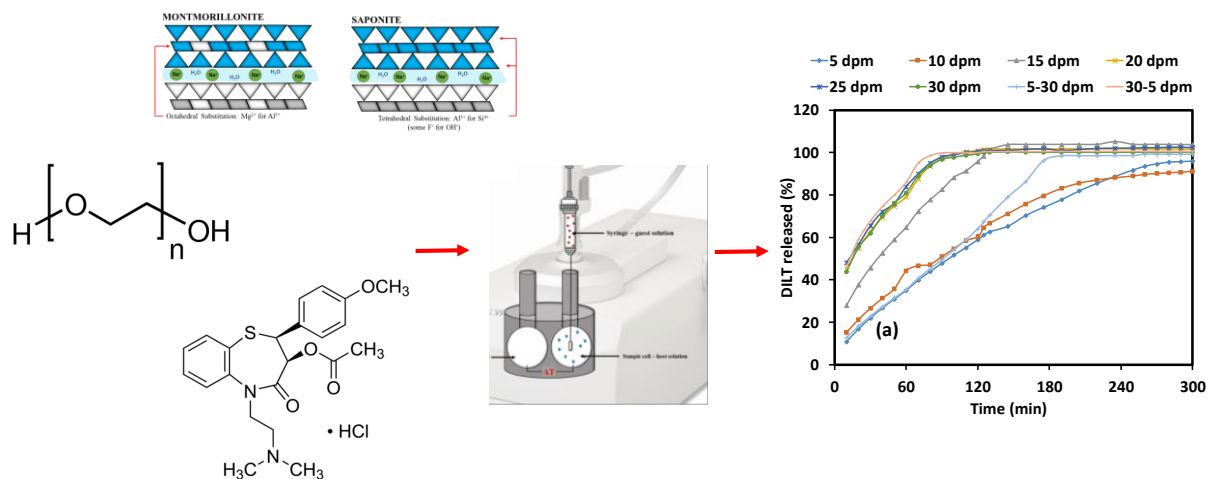
27 USP III used to successfully simulate fed and fasted states with matrices robust in up to 0.2 M
28 ionic strength

29

30

31 **Graphical abstract**

32



ISOTHERMAL CALORIMETRY IN UNDERSTANDING DRUG RELEASE FROM COMPLEXES

33

34

35

36 **Abstract**

37 This work investigated the use of the USP III apparatus in discriminating simulated fed and
38 fasted conditions as well as ionic strength on veegum-polyethylene (PEO) (called clay-PEO
39 matrices hereafter) matrices. The successful formulations were characterised using differential
40 scanning calorimetry (DSC) and evaluated for their physical properties. Isothermal calorimetry
41 (ITC) was used to evaluate the thermodynamics of the complexation processes. The effect of
42 agitation sequences on the matrices as evaluated from the USP III suggested an increase in
43 polymer content to significantly decrease the burst release experienced using diltiazem
44 hydrochloride (DILT) as a model cationic drug. The manufacturing methods showed superior
45 performance in relation to a decrease in burst release over the physical manufactured
46 counterparts. The clay-PEO matrices also showed robustness (no matrix failure) in up to 0.2 M
47 ionic strength solutions mimicking the upper limit experienced in the GI tract. ITC results
48 revealed that the binding between DILT and PEO was enthalpy and entropy-driven.
49 Furthermore, the binding between veegum and DILT in the presence of PEO was shown to be
50 enthalpy-driven and entropically unfavourable, which was also the case for the binding
51 between veegum and PEO thus giving insights to how the matrices were performing on a
52 molecular level.

53 **Keywords:** USP III apparatus; PEO, veegum; hydrophilic matrices; magnesium aluminium
54 silicate; nanocomposites

55 **Abbreviations:** PEO, polyethylene oxide; DSC, differential scanning calorimetry; MAS,
56 magnesium aluminium silicate; DILT, Diltiazem hydrochloride; ITC, Isothermal calorimetry;
57 PEG, polyethylene glycol; API, active pharmaceutical ingredient; NaCMC,
58 carboxymethylcellulose; PM, physical mixture; GI, gastrointestinal;

59

60 **1. Introduction**

61 Polyethylene oxide (PEO) (Figure 1a) is a synthetic polymer obtained commercially upon the
62 catalytic polymerisation of ethylene oxide. It has the same chemical structure as polyethylene
63 glycol (PEG) but a higher molecular weight, usually over 100,000. PEO is also soluble in a
64 wide variety of solvents (ethanol, acetone, toluene, chloroform) and in water. When dissolved
65 in water, PEO tablets hydrate, swell and form a gel layer outside the dry core. As with
66 hydrophilic matrices, this gel layer controls the release of an active pharmaceutical ingredient
67 (API) as the polymeric chains unfold and disentangle in the dissolution medium (Ward et al.,
68 2019; Nokhodchi et al., 2012; Ma, Deng and Cheng, 2014). Its physicochemical properties
69 such as rapid hydration and high water solubility, non-toxicity, pH insensitivity to
70 physiological fluids and easy manufacturability make PEO an attractive polymer and as such
71 it is widely used in the formulation of controlled drug release systems (Ma, Den and Cheng,
72 2014; Kim et al, 1995; Maggi et al., 2002; Shojaee et al., 2013a, 2013b, 2015; Kaialy et al.,
73 2016). Palmer et al. (2013) used PEO in combination with other matrix-forming polymers such
74 as sodium carboxymethylcellulose (NaCMC), to control the release of chlorpheniramine
75 maleate, venlafaxine hydrochloride, propranolol hydrochloride and verapamil hydrochloride
76 (Palmer et al., 2013). The authors found that a synergistic interaction between PEO and
77 NaCMC in the tablets significantly slowed drug release when compared to the tablets
78 containing a single polymer component (PEO or NaCMC) (Palmer et al., 2013; Nokhodchi et
79 al., 2015).

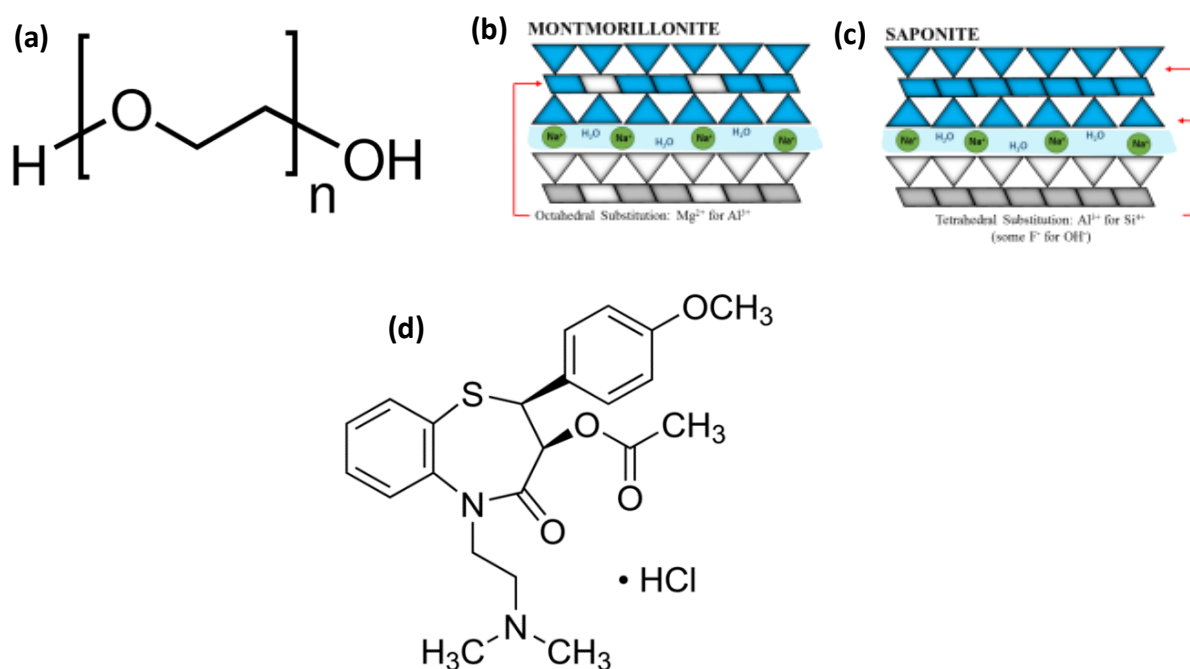
80 Veegum also known as magnesium aluminium silicate (MAS) (Figure 1b and c) is a mixture
81 of natural smectite montmorillonite and saponite clays. Veegum has a layered silicate structure,
82 formed of one alumina or magnesia octahedral sheet, sandwiched between two tetrahedral
83 silicate sheets (Vanderbilt 2014a and b; Kanjanakawinkul et al., 2013; Totea et al., 2020). MAS
84 has become a material for the use in drug formulation due to its high surface area and good

85 affinity with cationic drugs which has been well documented and exploited (Rojtanatanya and
86 Pogjanyakul., 2010; Adebisi *et al.*, 2015; Okeke and Boateng, 2016, 2017; Totea *et al.*, 2019).
87 Several polymers including quaternary polymethacrylates, chitosan and alginate have also been
88 successfully crosslinked with veegum to produce coatings, films or matrices for the successful
89 delivery of drugs (Rongthong *et al.*, 2013, 2020; Khuathan and Ponjanyaikul, 2014; Khlibsuwan
90 *et al.*, 2017; Khlibsuwan *et al.*, 2016). Pappa *et al.* reported the intercalation of PEO between
91 nanolayers of sodium montmorillonite to formulate nanostructured composites, intended for
92 the dissolution modulation of aprepitant. The authors found the PEO and clay nanocomposites
93 were highly effective as drug carriers for sustained release (Pappa *et al.*, 2018).

94 Diltiazem hydrochloride (DILT) (Figure 1d) is a non-dihydropyridine calcium channel blocker
95 with molecular weight and pKa of 450.98 g/mol and 7.8 respectively. DILT inhibits the calcium
96 channels in the blood vessels which leads to vasodilatation and, hence lower blood pressure
97 (Padial *et al.*, 2016). DILT has an elimination half-life of 3.2 ± 1.3 h following oral
98 administration with a bioavailability of 42 ± 18 % following first-pass metabolism (Herman *et*
99 *al.*, 1983) therefore making it an ideal candidate for extended release (Qazi *et al.*, 2013; Li *et*
100 *al.*, 2016) hence its use as the model cationic drug.

101 Although multiple studies have reported the efficient use of PEO as an excipient in the
102 formulation of controlled release systems on its own or in combination with other polymers or
103 materials such as clay, the effect of the polymer on the clay adsorption capacity has not been
104 previously explored at a molecular level. This experiment therefore aims to understand the
105 interactions between the model drug DILT, PEO and veegum at the molecular level and how
106 the interaction can potentially impact on the drug release from the clay-PEO matrices. This is
107 primarily investigated using isothermal calorimetry (ITC). Secondly, a more biorelevant
108 dissolution methodology (USP III) is utilised in conducting the dissolution studies using a
109 range of dip per minute (dpm) as well as dpm in ascending and descending order as reported

110 elsewhere (Asare-Addo et al., 2013a and b) to mimic the potential effect of food as well as
111 ionic strength on DILT release from the manufactured matrices. To the best of the author's
112 knowledge, this is the first of such a study. Hence, the information reported in this study will
113 allow a formulator to draw conclusions on parameters that may need to be manipulated in order
114 to improve drug release modulation.



115
116 Figure 1. Chemical structures of material used (a) Polyethylene oxide (PEO), (b) Magnesium
117 aluminium silicate (Veegum) and (c) Diltiazem hydrochloride.

118
119 **2. Materials and methods**

120 **2.1 Materials**

121 The hydrophilic matrix tablets were prepared using DILT as the model drug. DILT was
122 purchased from TCI chemicals, UK. The PEO (Polyox WSR 301, with a molecular 4,000,000)
123 polymer was a kind gift from Colorcon, Ltd, UK. Veegum F was a kind gift from Lake
124 Chemical UK. The dissolution media used was prepared according to the USP 2003 method of
125 preparing buffers using potassium chloride (Acros Organic, UK), hydrochloric acid (Fisher

126 Scientific, UK) for pH 1.2 and 2.2, and potassium phosphate monobasic-white crystals (Fisher
127 BioReagents, UK) and sodium hydroxide (Fisher Scientific, UK) for pH 5.8, 6.8, 7.2 and 7.5
128 media.

129 When investigating the effect of ionic strength on the drug release, sodium chloride (Fisher
130 Scientific, UK) was used to adjust the ionic strength of each pH buffer.

131

132 **2.2 Tablet preparation and mechanical strength test**

133 Six formulations in total were prepared in three distinct ways to aid comparisons. The first two
134 formulations (F1 and F2) were prepared by measuring out the components as in [Table 1](#) and
135 mixed in the Turbula blender (Type T2C, Switzerland) for 10 min (these two formulations are
136 classified as the physical mixtures (PM)). For formulations F3 and F4, the drug (DILT) was
137 firstly dissolved in deionised water (5 mL) after which it was added to the veegum in a ball
138 mill (10 min at 400 rpm). After this was air-dried, it was mixed with the appropriate amount of
139 PEO in the turbula mix for 10 min. Formulation F5 and F6 were prepared by physically mixing
140 the veegum and DILT in the turbula mix for 10 min, introducing the clay-drug mix into the ball
141 mill (10 min at 400 rpm) then adding deionised water (5 mL) to the milling process. After the
142 drying process, the appropriate amount of PEO was again added and mixed on the turbula mix
143 for 10 min ([Table 1](#)). Round cylindrical tablets with a diameter of 9.6 mm (obtained using an
144 electronic digital calliper) with a target weight of 250 mg were then prepared ([Table 1](#)) using
145 a single punch tableting machine at 1500 psi (5.5 kN) (Model MTCM-1, Globe Pharma, US).
146 The die wall was lubricated each time before tablet compression using a 2 % suspension of
147 magnesium stearate in acetone to enable the easy removal of the tablets from the die.

148 As an additional investigation, the hardness of the compressed tablets was explored to aid
149 comparisons between the various formulations. Using a tablet hardness tester (Model 8M),

150 tablets were fractured diametrically with the result displayed in Newton (N) on the screen and
151 recorded. All experiments were conducted in triplicate

152 Table 1. Composition for each formulation (values are per tablet)

Formulation code	Initial process	Diltiazem HCl (mg)	Veegum (mg)	PEO 301 (mg)	Nominal weight (mg)
F1	Simple physical mixture of all components in turbular blender	200	25	25	250
F2	Simple physical mixture of all components in turbular blender	200	16.7	33.3	250
F3	Drug was dissolved in water and mixed with veegum in ball mill. After drying, the mixture was mixed with PEO	200	25	25	250
F4	Drug was dissolved in water and mixed with veegum in ball mill. After drying, the mixture was mixed with PEO	200	16.7	33.3	250
F5	Drug and veegum was mixed uniformly following by grinding in ball mill in the presence of water. After drying the mixture was mixed with PEO	200	25	25	250
F6	Drug and veegum was mixed uniformly following by grinding in ball mill in the presence of water. After drying the mixture was mixed with PEO	200	16.7	33.3	250

153

154 2.3 Carr's Index

155 The tap and bulk densities were determined according to the method of [Nep et al., 2017](#) for the
156 formulations produced (F1-F6) to allow the determination of their Carr's Compressibility
157 Index (%) (Equation 1). In brief, 10 g of each of the formulation was introduced into a 100 mL
158 measuring cylinder. Taking care not to disturb the cylinder, the volume was read to give the
159 bulk volume of the powder tested. The measuring cylinder was then tapped until the volume

160 of powder was constant representing the tapped volume. The bulk or tapped density was then
161 calculated. experiments were conducted in triplicates.

162

$$163 \quad CI = \left(\frac{Pt - Pb}{Pt} \right) \times 100 \quad \text{Equation 1}$$

164 where;

165 CI = Carr's Index, Pb = Bulk Density and Pt = Tapped Density

166

167 **2.4 Differential Scanning Calorimetry (DSC)**

168 DSC was used as an investigation to evaluate the composition of the formulation to see if there
169 were any interactions between the drug and polymers after mixing and heating. Samples of
170 each formulation, as well as samples of the pure materials only (DILT, PEO and Veegum),
171 were placed in a standard 40 µm aluminium crucibles and sealed. These aluminium crucibles
172 were heated from 25 to 300 °C at a scanning rate of 10°C/min under nitrogen gas using a
173 Mettler Toledo DSC equipment. The software provided by the instrument was used to evaluate
174 the melting point and enthalpy were recorded.

175

176 **2.5 Dissolution studies**

177 *2.5.1 Effect of dip rate on the release of DILT from the clay-PEO matrices*

178 An automated USP type III Bio-Dis (Varian, US) was used to carry out the dissolution tests.
179 For the first two formulations (F1 and F2), agitation rates of 5, 10, 15, 20, 25, 30, 5-30
180 (ascending order) and 30-5 dpm (descending order) were evaluated as shown in [Table 2 \(Asare-](#)
181 [Addo et al., 2010\)](#). The transit times in [Table 2](#) represents the period of time the tablet matrix
182 stays in a particular vial before transferring to the next vessel. The changes in pH as in [Table 2](#)
183 were used to simulate the digestive tract ([Klein et al., 2002](#)). Following this, for the remaining

184 formulations (F3-F6) was evaluated at a dip rate 20 dpm only for comparison. The dissolution
 185 vessels contained 250 mL of the appropriate medium and the temperature of the medium was
 186 kept constant at 37 ± 0.5 °C. DILT release was measured using a UV/visible spectrophotometer
 187 at a wavelength of 240 nm.

188 *2.5.2 Effect of ionic strength on the release of DILT from the clay-PEO matrices*

189 To investigate the effect of ionic strength on DILT release from the matrices, sodium chloride
 190 was used to regulate the ionic strength at 0.2 M in buffers with pH of 1.2, 2.2, 5.8, 6.8, 7.2 and
 191 7.5 (Asare-Addo et al., 2011). All formulations (F1-F6) were tested using this methodology to
 192 investigate potential differences between the formulations as they were subjected to the
 193 different ionic strength conditions.

194

195 Table 2. Transit times, pH values and agitations applied during dissolution testing of DILT
 196 clay-PEO matix tablets

Media pH	Transit time (min)	Applied Agitation (dpm)							
		Constant						Ascending	Descending
1.2	60	5	10	15	20	25	30	5	30
2.2	60	5	10	15	20	25	30	10	25
5.8	10	5	10	15	20	25	30	15	20
6.8	120	5	10	15	20	25	30	20	15
7.2	30	5	10	15	20	25	30	25	10
7.5	30	5	10	15	20	25	30	30	5

197

198 *2.5.3 Mathematical modelling of drug release*

199 There have been several equations reported in literature used in mathematical modelling to
200 define the mechanisms of drug release (Bruschi 2015; Gonçalves-Araújo et al., 2010). Two
201 different models namely, Higuchi and the Korsmeyer–Peppas model (Power Law) (Equations
202 1 and 2 respectively) are adopted here to aid in defining the mechanisms arising as a result of
203 the varying agitation or increased ionic strength.

$$204 \quad Q = K_{HT}t^{0.5} \quad \text{Equation 1}$$

$$205 \quad Q = K_{KT}t^n \quad \text{Equation 2}$$

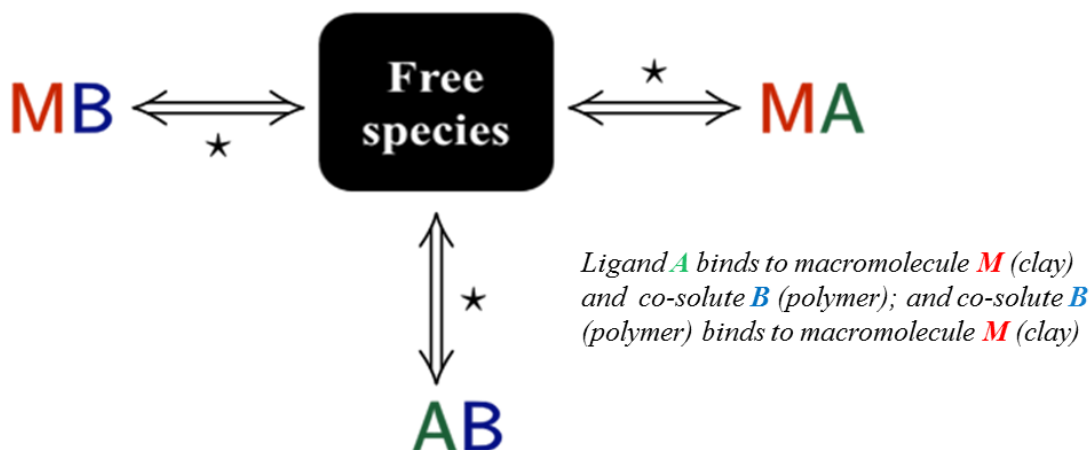
206 In these equations, Q is the amount of the drug dissolved in time t; K_H is the Higuchi rate
207 constant; K_K is the release constant and n is diffusional exponent. As the compacts produced
208 were cylindrical, n values of up to 0.45 suggest Fickian diffusion, and values of above 0.89
209 suggest Case-II transport. Value between these two suggests anomalous transport (Ford et al.,
210 1991; Siah-Shadbad et al., 2011). For a detailed review of these processes, readers are referred
211 to the following citations (Siepmann and Peppas 2001, 2012; Bruschi, 2015).

212

213 **2.6 Isothermal calorimetry (ITC) - effects of PEO on the adsorption of DILT onto veegum**

214 The molecular interactions between DILT and veegum has been recently explored and
215 published by the authors (Totea et al., 2020). The authors of the current research therefore
216 focused on understanding the interactions between DILT, veegum and PEO in this manuscript.
217 To this end, calorimetric studies were carried out at 25 °C and pH 5, to study the effects of
218 PEO on veegum-DILT binding. Experiments were undertaken between PEO and veegum, PEO
219 and DILT, as well as DILT and veegum-PEO mixture. Control binding studies were also
220 performed. The binding isotherm was studied in 30 – 35 injections of 8 – 10 µL each into the
221 sample cell every 550 – 1500 seconds. Veegum dispersion (0.037 % w/v) and DILT solution
222 (0.090 % w/v (2 mM)) were prepared. PEO dispersion (0.020 – 0.037 % w/v) was also
223 prepared. The veegum-PEO mixture was prepared using a 1:1 v/v mixture of separately

224 prepared veegum dispersion (0.074 % w/v) and PEO dispersion (0.040 % w/v). A competitor
225 binding model (Figure 2) was fitted to the data to determine thermodynamic parameters using
226 AFFINImeter (AFFINImeter, Spain).



227
228 Figure 2. Competitive ligand binding where A is the ligand in the syringe (DILT) and M and
229 B are the macromolecule and co-solute respectively (Veegum and PEO respectively), both
230 present in the sample cell.

231

232 3. Results and discussion

233 3.1 Solid-state properties and physical properties of the starting materials and formulated 234 blends

235 The DSC thermograph of the pure drug DILT exhibited a sharp endothermic melting peak at ~
236 209 °C (Table 3). Prasad *et al.*, 2013, however, reported the melting peak of DILT to be around
237 ~ 215 °C. This difference may have to do with the manufacturing and purity of the drug as they
238 were sourced from different suppliers. The veegum exhibited a broad endothermic peak at ~
239 70 °C, which was attributed to the dehydration of free water residues within the clay (Figure
240 3a) which has also reported elsewhere (Rojtanatanya and Pongjanyakul, 2010). PEO exhibited
241 a broad melting peak at ~ 66 °C due to its crystalline structure (Figure 3a) (Ozeki *et al.*, 1999;

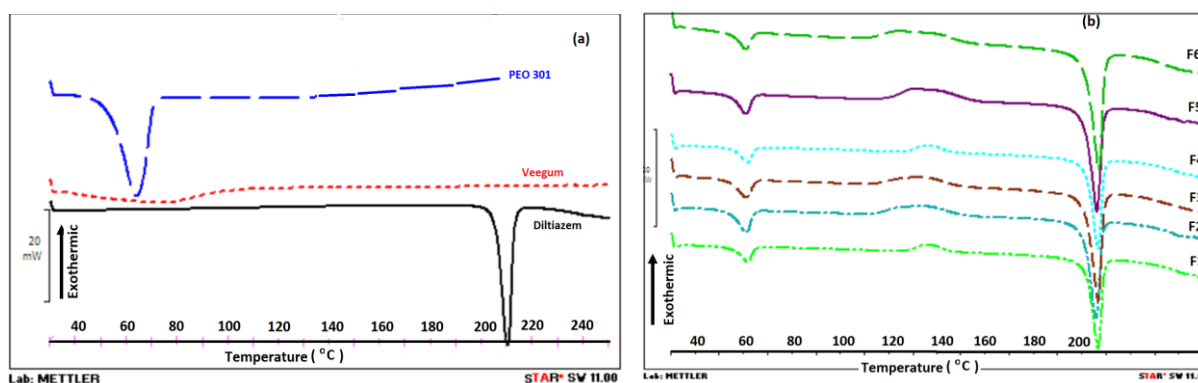
242 Crowley *et al.*, 2002). All formulations exhibited the crystalline peak for PEO, however, there
243 was a slight decrease in the melting point of the DILT present therein. The melting points of
244 DILT in the formulations ranged between 204 - 206 °C (Table 3). These deviations in the
245 melting point in the formulations coincided with significant decreases in the enthalpy of the
246 DILT in the formulations. Pure DILT had an enthalpy of ~ 106 J/g which dropped to range
247 from 79 – 85 J/g (Table 3) suggesting a decrease in the crystallinity of DILT in the various
248 formulations. This behaviour has been observed and reported for propranolol hydrochloride, a
249 cationic drug used in the liquisolid preparation for veegum-polysaccharide matrices (Ward *et*
250 *al.*, 2020). The preparation methods for the formulation (F3-F6) where the DILT drug was
251 mixed with the veegum in the presence of water or DILT dissolved in water first and mixed
252 with the veegum (Table 1) causes an intercalation of the cationic drug between the layers of
253 the veegum (Rojtanatanya and Pogjanyakul., 2010). This process molecularly disperses some
254 of the drug which may also be accountable for the reduction in the observed enthalpy. For the
255 physical formulations (F1 and F2), it is also possible that the observed decrease in the enthalpy
256 for the DILT peak may be caused by a solubilisation of the DILT crystals in the melted PEO
257 which may also cause some of the DILT to be in amorphous form (Kaialy *et al.*, 2016; Alhijjaj
258 *et al.*, 2015).

259 The Carr's index for flowability did not show any real trends with values ranging from 22 – 30
260 indicating fair to poor flowability for the formulations (Table 3). This, however, did not impact
261 on the tableting process as a single punch tableting instrument was used. It was also
262 interesting to note that processing associated with the manufacture of the formulation F3-F6
263 did not impact greatly on the hardness of the compacts produced.

264 Table 3. Carr's index, formulation compact hardness and DSC traces for enthalpy and melting
265 of DILT in each manufactured formulation.

Formulation code	Carr's index (%)	Hardness (N)	Enthalpy (J/g)	Melting (°C)
DILT	-	-	106.2±1.6	208.9±0.8
F1	24.3±4.7	28.0±1.0	81.4±1.6	206.0±0.8
F2	29.4±1.0	31.3±1.5	84.1±5.0	204.6±0.4
F3	29.5±1.1	34.6±1.5	82.0±8.9	205.3±0.1
F4	28.0±2.4	29.6±0.6	80.2±11.5	204.1±0.9
F5	21.9±1.0	31.0±1.7	84.7±4.6	205.8±0.9
F6	25.2±1.0	36.6±0.6	79.3±3.9	205.8±0.4

266



267

268 Figure 3. DSC thermographs of (a) starting materials, PEO, veegum and DILT drug, (b)
 269 manufactured formulations for making compacts for dissolution testing. For an understanding
 270 of the formulation code, please refer to Table 1. Note: Black arrow indicates exothermic
 271 direction.

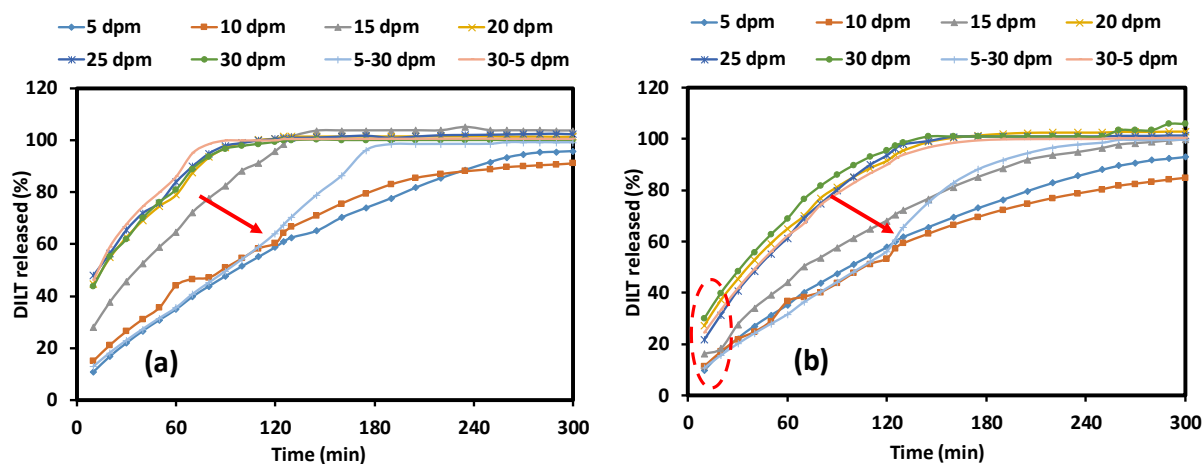
272 3.2 Effect of agitation on DILT release

273 The method of increasing agitation (dpm) to mimic different food effect on matrices as
 274 developed by [Asare-Addo et al., \(2010\)](#) was used in discriminating against the clay-PEO
 275 matrices. It was interesting to note from [Figure 4](#) where the physical mixtures are investigated
 276 that generally, the lower agitations (5 and 10 dpm) showed similarity. Similarly, the higher
 277 agitations (20 – 30 dpm) were similar. This may seem to suggest that the hydrodynamics
 278 produced and the effects on the matrices at that set dpm could be similar. This may, however,
 279 require further studies to establish this fact around the influence of hydrodynamics. It is also

280 important to note that this behaviour may be polymer dependent (Asare-Addo *et al.*, 2013). Of
281 interest also is the profiles of the ascending order (where agitation is increased by 5 dpm every
282 time the cylinder containing the formulation is moved from one vial to the other. This means
283 in pH 1.2, the agitation is 5 dpm, 10 dpm in pH 2.2, 15 dpm in pH 5.8, 20 dpm in pH 6.8, 25
284 dpm in pH 7.2 and finally 30 dpm in pH 7.5) and descending order (where the reverse
285 experimentation was conducted i.e. agitation was decreased by 5 dpm every time the cylinder
286 containing the formulation moved from one vial to the other meaning in pH 1.2, agitation was
287 kept at 30 dpm, in pH 2.2, agitation was kept at 25 dpm and so forth) of agitations. Here it was
288 observed that at the descending order of agitation, the drug release profile was similar to that
289 of the higher agitation (20-30 dpm) profiles with the drug all going into solution around 90-
290 100 min (Figure 4a) or around 130-145 min (Figure 4b). Where the ascending order of agitation
291 is concerned, the lower agitation profiles of 5 and 10 dpm is followed closely till around the
292 120 min mark where agitation is set to now move to 15 dpm (indicated by the red arrow in
293 Figure 4). Here, it is possible that the gel layer formed is decreasing as a greater level of
294 agitation is applied and therefore erosion increased hence the sudden increase in drug release.
295 The different profiles obtained can, therefore, give an indication as to how different food effects
296 can influence drug release without the laboursome and often expensive methods of using actual
297 food in the dissolution testing method. In Table 4, the Higuchi and the Peppas (Power Law)
298 are applied to the release profiles. With the exceptions of drug release profiles from F2 at 10
299 and 15 dpm where the mathematical models suggested first order and the Higuchi as the
300 kinetics of release, all the dpms explored for both formulations (F1 and F2) had the Peppas
301 (Power Law) as the dominant kinetics of drug release. For the F1 matrices, the n values, where
302 the lowest agitation of 5 dpm was applied, anomalous transport was suggested to be occurring
303 with a value of 0.69. An increase in agitation or the dpm displayed a decrease in the value of n
304 up to the 20 dpm mark. This also suggested an increase in the contribution of Fickian diffusion

305 to accompany the increased agitation (Table 4). The ascending and descending order of
306 agitation had a significant impact on the n values (0.64 and 0.36 respectively). These values
307 suggested that when agitation is started of slowly (5 dpm), anomalous transport dominated
308 whereas when agitation is faster initially (30 dpm), Fickian diffusion dominates (Table 4).

309 [Figure 4](#) also signifies the phenomena where an increase in polymer content (PEO in this case)
310 significantly reduces the burst release. This observation has been recorded by several authors
311 for hydrophilic polymers ([Ebube et al., 1997](#); [Velasco et al., 1999](#); [Mason et al., 2015](#)).
312 Doubling the polymer content reduces the burst release experienced by the higher dpm profiles
313 (20-30 dpm), where over 40 % of the drug is released immediately ([Figure 4a](#)) to less than 30
314 % for these same dpm experiments ([Figure 4b](#)). This is indicated by dashed red lines in [Figure](#)
315 [4b](#). This observed decrease is also explained further with the ITC data in section 3.4 where the
316 interactions between PEO, DILT and veegum is thought to have a contributory factor. Here
317 also (F2), there was a decrease in the n value that accompanied an increase in the level of
318 agitation from 5 dpm – 20 dpm (Table 4). In this case however, the increase in the polymer
319 content meant there was more of a contribution of swelling as indicated by their increased n
320 values (Table 4). The ascending and descending order of agitation both displayed anomalous
321 transport with n values of 0.67 and 0.52 respectively suggesting that when agitation is started
322 of slowly, swelling tends to contribute a lot more than when agitation is faster initially (Table
323 4).



324

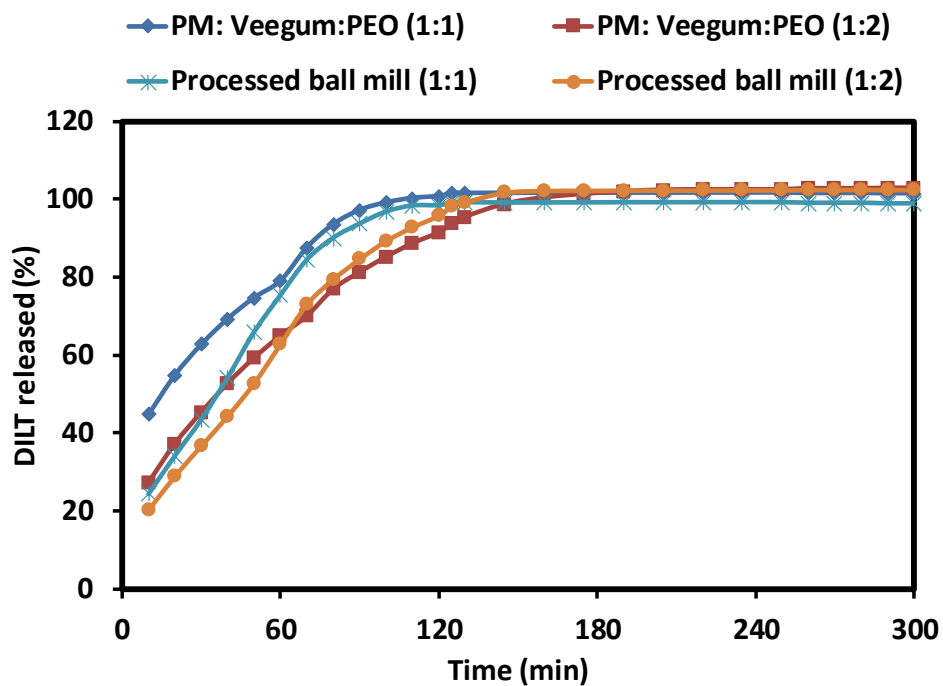
325 Figure 4. Dissolution profiles of DILT from the physical mixture formulations (PM) (a) F1-
 326 containing veegum:PEO in a 1:1 ratio respectively, (b) F2 - containing veegum:PEO in a 1:2
 327 ratio respectively assessing the effects of agitation (dpm) on the manufactured matrices

328 Table 4. Mathematical models used in evaluating drug release profiles from the formulations
 329 at the varying agitations

Formulation and dipping speed (dpm)	Mathematical model			Formulation and dipping speed (dpm)	Mathematical model		
		RSQ	k		n	RSQ	k
F1-5dpm	Higuchi	0.9949	0.0647	F2-5dpm	0.9955	0.0619	
	Peppas (Power Law)	0.9987	0.0216		0.69	0.9996	0.0192
F1-10dpm	Higuchi	0.9777	0.0573	F2-10dpm	0.9888	0.0551	
	Peppas (Power Law)	0.9925	0.0389		0.57	0.9940	0.0245
F1-15dpm	Higuchi	0.9971	0.0898	F2-15dpm	0.9836	0.0642	
	Peppas (Power Law)	0.9988	0.0957		0.46	0.9672	0.0333
F1-20dpm	Higuchi	0.9944	0.0822	F2-20dpm	0.9980	0.0835	
	Peppas (Power Law)	1.0000	0.2286		0.29	0.9986	0.0890
F1-25dpm	Higuchi	0.9517	0.0760	F2-25dpm	0.9964	0.0938	
	Peppas (Power Law)	0.9987	0.0730		0.53	0.9987	0.0555
F1-30dpm	Higuchi	0.9656	0.0708	F2-30dpm	0.9961	0.0864	
	Peppas (Power Law)	1.0000	0.2012		0.34	0.9979	0.1061
F1-5-30dpm	Higuchi	0.9471	0.0708	F2-5-30dpm	0.9621	0.0736	
	Peppas (Power Law)	0.9895	0.0270		0.64	0.9925	0.0210
F1-30-5dpm	Higuchi	0.9695	0.0782	F2-30-5dpm	0.9787	0.0784	
	Peppas (Power Law)	1.0000	0.2034		0.36	0.9958	0.0728

330

331 In Figure 5, the PM formulations F1 and F2 are compared to formulations F5 and F6 where the
 332 DILT and veegum were mixed together in a turbula mixer before being ground together in a
 333 ball mill in the presence of water, dried and finally mixed with PEO. In the case of F1 and F5
 334 where the veegum and PEO are in the 1:1 ratio, it was evident that the processing of F5 brought
 335 about a significant decrease in the burst release profiles at 20 dpm. The burst release
 336 experienced by F1 at 45 % was reduced to 24 %. Although a decrease was also observed by
 337 the F6 formulation in comparison to its PM counterpart F2, it was not as poignant as the effects
 338 of the increased polymer content come to effect here. Further explanation as to the behaviour
 339 observed as a result of the processing parameters will be explored in section 3.4.

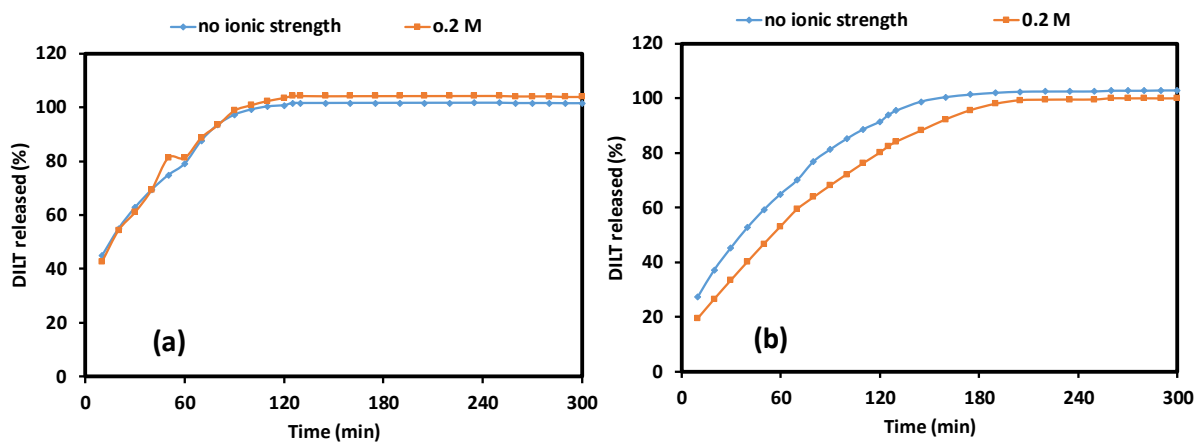


340

341 Figure 5. Dissolution profiles of DILT from the physical mixture formulations (PM) F1 and F2
 342 being compared to the processed balled milled samples. Note: processed ball milled samples
 343 here refer to formulation F5 and F6 and dissolution was conducted at an agitation of 20 dpm
 344

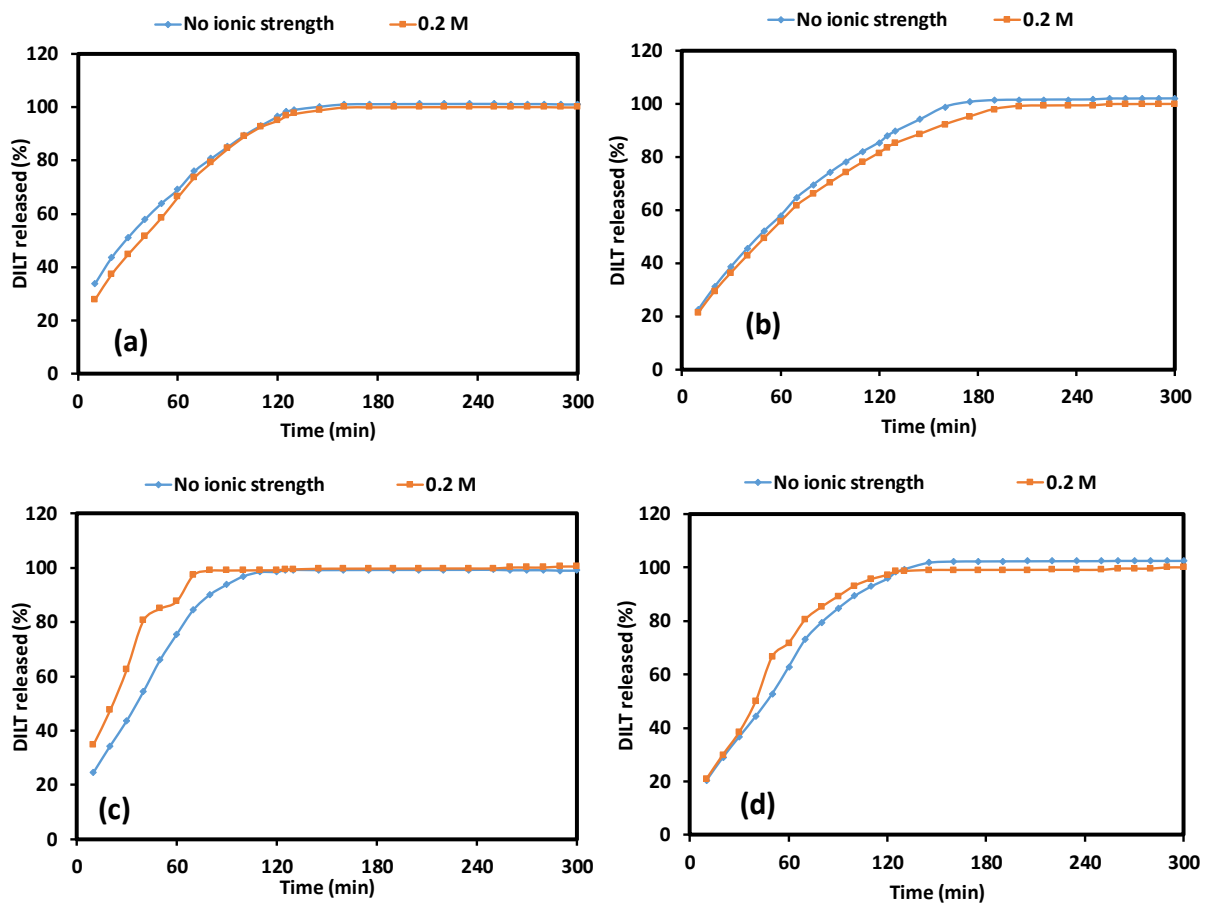
345 **3.3 Effect of ionic strength on DILT release**

346 pH and ionic strength are two of the major properties of the gastrointestinal (GI) fluids and are
 347 reported to vary greatly along the GI tract under fasting and fed conditions (Charman *et al.*,
 348 1997, Wilson and Washington, 1989). It has been estimated that in a fasted stomach, ionic
 349 concentration strength is approximately 0.11 M (Lindahl *et al.*, 1997). As a result, ionic
 350 concentrations of up to 0.2 M is tested to determine the robustness of the clay-PEO matrices.
 351 Figure 6 depicts the effect of ionic strength on the PM formulations F1 and F2. Here, Figure
 352 6b shows a reduction in the burst release experienced by the clay:PEO in the 1:1 ratio. This in
 353 fact, is also experienced by the formulation F3-F6 (Figure 7) although formulation F3 and F5
 354 experience reduced burst effect in comparison to their PM counterpart F1 due to their
 355 manufacturing process. Here also, a further increase in the polymer content brings about a
 356 further decrease in burst release. The similarity in release profiles also suggests that these
 357 matrices are robust to the effect of ionic strength.



358
 359 Figure 6. Dissolution profiles of DILT from the physical mixture formulations (PM) (a) F1-
 360 containing veegum:PEO in a 1:1 ratio respectively, (b) F2 - containing veegum:PEO in a 1:2
 361 ratio respectively assessing the effects of ionic strength at an agitation of 20 dpm
 362 Table 5 displays the mathematical models used in the analysis of the release profiles in ionic
 363 media of 0.2 M NaCl. The physical mixture formulation show that F1 has Fickian diffusion as
 364 a dominant mechanism whereas the increased polymer content for the F2 formulation suggests

365 anomalous transport as the dominant mechanism. It was also interesting to note that F3 and F5
366 both had the Peppas (Power Law) as the main dominant mechanism whereas the F4 and F6
367 formulation (increased polymer content) had Higuchi as the dominant mechanism. The
368 reported values of n however when the Peppas model is applied (0.53 and 0.62) depicts how a
369 small change in the formulation process can significantly impact the kinetics of release
370 suggesting care and consideration being given to these investigated parameters (Table 5).



371

372 Figure 7. Dissolution profiles of DILT from the formulations (a) F3 - containing veegum:PEO
373 in a 1:1 ratio respectively, (b) F4 - containing veegum:PEO in a 1:2 ratio respectively (c) F5 -
374 containing veegum:PEO in a 1:1 ratio respectively, (d) F6 - containing veegum:PEO in a 1:2
375 ratio respectively assessing the effects of ionic strength at an agitation of 20 rpm

376 Table 5. Mathematical models used in evaluating drug release profiles from the formulations
 377 in the ionic strength media (0.2 M) at 20 dpm only.

Formulation	Mathematical model			Formulation	Mathematical model		
	RSQ	k	n		RSQ	k	n
F1	Higuchi	0.9911	0.0892	F2	0.9969	0.0822	
	Peppas (Power Law)	1.0000	0.1900		0.35	0.9912	0.0524
F3	Higuchi	0.9929	0.1005	F4	0.9963	0.0809	
	Peppas (Power Law)	0.9990	0.1068		0.45	0.9958	0.0635
F5	Higuchi	0.5452	0.0224	F6	0.9814	0.1299	
	Peppas (Power Law)	0.9867	0.0921		0.52	0.9859	0.0534

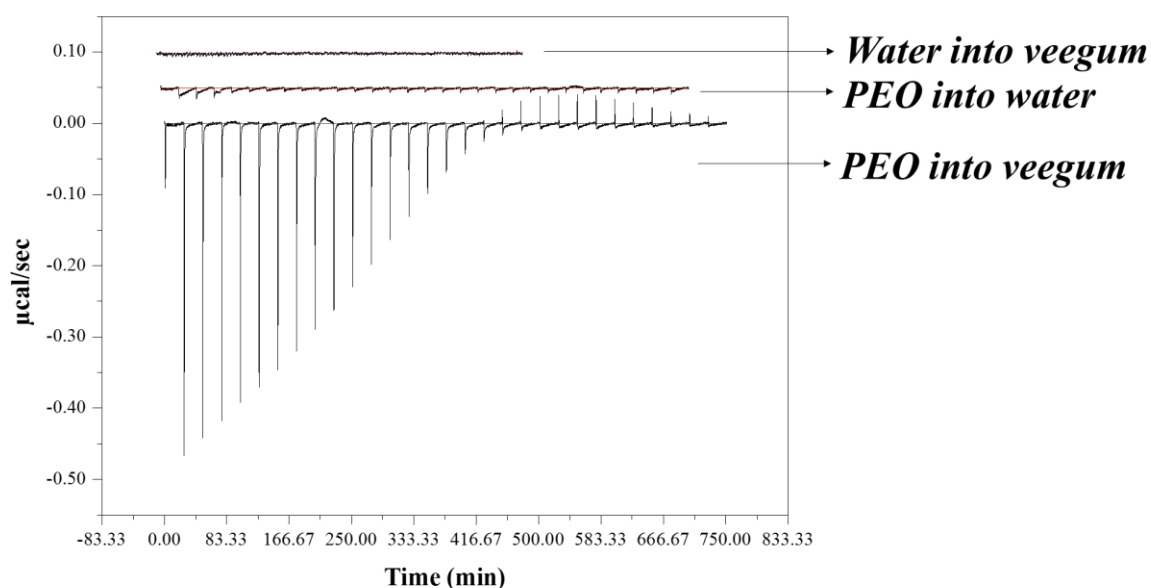
378

379 3.4 ITC in understanding the effects of PEO on the adsorption of DILT onto MAS

380 It has been reported that cationic drugs intercalate between the layers of veegum or MAS
 381 ([Rojtanatanya and Pongjayakul 2010](#)). This property has been exploited in the modulation of
 382 drug release as well as in the preparation of nanocomposites for film coatings ([Rongthong et](#)
 383 [al., 2020](#); [Pongjanyakul et al., 2013](#)). [Totea et al., 2019 and 2020](#) recently detailed the
 384 thermodynamics of two cationic drugs binding to veegum. The authors found using propranolol
 385 hydrochloride as a model drug that the overall change in enthalpy was exothermic with a
 386 comparatively small entropic contribution to the total change in Gibbs free energy ([Totea et](#)
 387 [al., 2019](#)). This suggested that the binding process was enthalpically driven and entropically
 388 unfavourable meaning hydrogen bonding and electrostatic interactions dominating the
 389 interaction. For DILT, the same authors found that a competitor binding model was needed and
 390 therefore proposed one which suggested from the thermodynamics that DILT binding to
 391 veegum was thought to enthalpy driven and entropically unfavourable ([Totea et al., 2020](#)).

392 From the ITC studies conducted, the interaction between veegum and PEO at 25 °C was shown
 393 to be exothermic in nature. The non-constant heats and non-sigmoidal curve suggested that
 394 PEO can weakly bind to veegum and form a complex by intercalation of PEO particles between
 395 the veegum platelets ([Figure 8](#)) ([Gao, 2004](#)). The binding isotherm showed non-constant heats
 396 at the end of titration in the presence of excess PEO. This could be due to the aggregation of

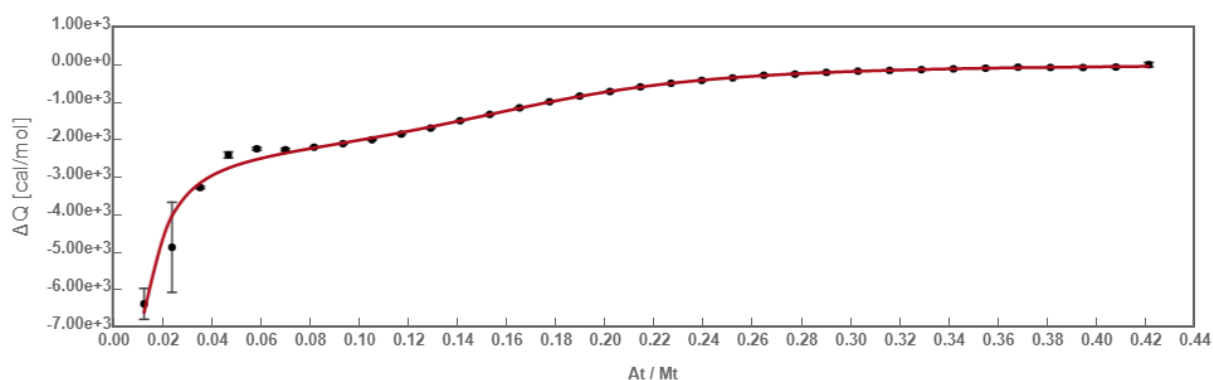
397 the PEO-veegum mixture or a contribution of the PEO self-aggregation in water at pH 5. PEO
398 dilution into water at pH 5 (25 °C) (Figure 8) showed a monotonous decrease of ITC heat
399 signals without a sigmoidal behaviour, suggesting that PEO self-associates weakly in aqueous
400 solution. Due to its amphiphilic structure (hydrophobic backbone and hydrophilic side groups),
401 PEO may show a tendency to self-aggregate in aqueous solution, even at a very low
402 concentration.



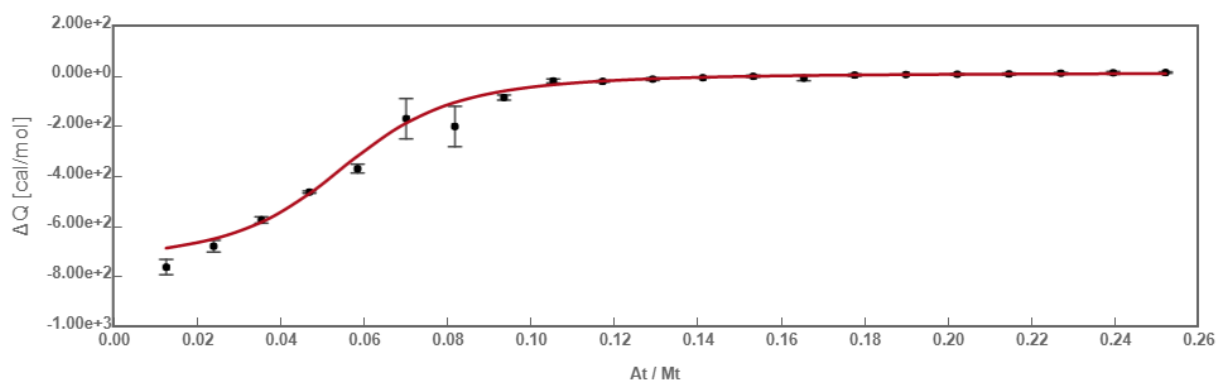
403
404 Figure 8. Raw data for titration of 0.037 % w/v PEO dispersion (pH 5) into 0.037 % w/v
405 veegum dispersion (pH 5) at 25 °C; Control run between 0.037 % w/v PEO dispersion solution
406 (pH 5) and water (pH5) at 25 °C and between 0.037 % w/v veegum dispersion solution (pH 5)
407 and water (pH5) at 25 °C.

408 To study the effects of PEO on veegum-DILT binding, the simple binding experiment between
409 DILT and PEO (Figure 9) was linked to the data showing the effects of PEO on DILT
410 adsorption onto veegum (Figure 10). Hence, a competitive binding model was fitted to the data
411 showing the binding between veegum, DILT and PEO, using the parameters obtained
412 following the fitting of a one set of sites model to the data showing DILT and PEO binding.

413 Results showed that the binding between DILT and PEO was enthalpy and entropy driven
414 (Table 6). Furthermore, the binding between veegum and DILT in the presence of PEO was
415 shown to be enthalpy driven and entropically unfavourable, which was also the case for the
416 binding between veegum and PEO (Table 6). This behaviour suggests that the entropic effects
417 observed in the simple veegum-DILT binding experiment (negative $-T\Delta S$) are reduced upon
418 the addition of the polymer to the mixture.



419
420 Figure 9. Thermodynamic profile through a competitive curve fitting model for adsorption of
421 DILT solution (0.090 % w/v (2 mM)) pH 5 onto veegum-PEO mixture (0.037 % w/v veegum
422 and 0.020 % w/v PEO mixed together at a ratio of 1:1 v/v) pH 5 at 25 °C



423
424 Figure 10. Thermodynamic profile through a one set of sites curve fitting model for adsorption
425 of DILT solution (0.090 % w/v (2 mM)) pH 5 onto PEO dispersion (0.020 % w/v) pH 5 at 25
426 °C

427 Table 6. Calorimetric binding studies evaluating the adsorption of DILT (0.090 % w/v (2 mM))
 428 onto veegum (0.036 % w/v) at 25°C (pH 5). Data analysed through a competitive curve fitting
 429 model to calculate affinity (K) and changes in enthalpy (ΔH) and entropy ($-T\Delta S$).

Reaction	r	K_a [M ⁻ⁿ]	H [cal/mol]	-TΔS [cal/mol]
M + A ↔ MA	0.06	5.2897E+5 ± 4.7516E+4	-6.9949E+4 ± 7.8197E+3	6.23E+04
*A + B ↔ AB	0.05	1.7682E+5 ± 1.9010E+3	-8.6260E+2 ± 5.4944E+0	-6.19E+03
M + B ↔ MB	0.06	8.7715E+5 ± 1.1242 E+5	-6.8785E+4 ± 7.8152E+3	6.08E+04

430 *binding parameters for DILT binding to PEO

431

432 The findings therefore imply that both veegum and PEO will compete for the binding with
 433 DILT which, in turn, will have effects on DILT release from the veegum-PEO matrices in
 434 slowing DILT release. Furthermore, due to the interaction observed between PEO and MAS it
 435 is expected that during DILT dissolution from veegum-PEO matrices, some of the sites on
 436 veegum would become saturated with PEO, which would prevent readsorption of DILT on
 437 both veegum and PEO.

438

439 4. Conclusions

440 Veegum-PEO matrices were successfully manufactured using different manufacturing
 441 techniques. The effect of agitation sequences on the matrices suggested an increase in polymer
 442 content to significantly decrease the burst release experienced using diltiazem hydrochloride
 443 as a model cationic drug. The manufacturing methods showed superior performance in relation
 444 to a decrease in burst release over the physical manufactured counterparts. The veegum-PEO
 445 matrices also showed resilience or robustness in up to 0.2 M ionic strength solutions mimicking

446 the upper limit experienced in the GI tract. ITC results revealed that the binding between DILT
447 and PEO was enthalpy and entropy-driven. Furthermore, the binding between veegum and
448 DILT in the presence of PEO was shown to be enthalpy-driven and entropically unfavourable,
449 which was also the case for the binding between veegum and PEO thus giving insights to how
450 the matrices were performing on a molecular level.

451

452 **Acknowledgements**

453 The authors are grateful to the Universities of Huddersfield and Sussex for funding. The authors
454 also thank Laura Waters of the University of Huddersfield, Irina Dorin formerly of Malvern
455 Panalytical, UK and Juan Sabin of AFFINImeter, Spain for useful discussions and help with
456 the ITC experiments.

457

458 **Author Contributions**

459 Kofi Asare-Addo: Conceptualisation; Writing—Original Draft; Writing—Review & Editing;
460 Data curation

461 Ana-Maria Totea: Data curation; Formal analysis; Methodology; Investigation

462 Ali Nokhodchi: Conceptualisation; Data curation; Methodology; Investigation; Writing—
463 Review & Editing

464

465 **Conflicts of Interest**

466 The authors declare no conflict of interest.

467

468

469

470 **References**

- 471 Adebisi, A. O., Conway, B. R., & Asare-Addo, K. (2015). The influence of fillers on
472 theophylline release from clay matrices. *American Journal of Pharmacological Sciences*, 3(5),
473 120-125.
- 474 Alhijaj, M., Bouman, J., Wellner, N., Belton, P., & Qi, S. (2015). Creating drug solubilization
475 compartments via phase separation in multicomponent buccal patches prepared by direct hot
476 melt extrusion–injection molding. *Molecular pharmaceutics*, 12(12), 4349-4362.
- 477 Asare-Addo, K., Levina, M., Rajabi-Siahboomi, A. R., & Nokhodchi, A. (2010). Study of
478 dissolution hydrodynamic conditions versus drug release from hypromellose matrices: the
479 influence of agitation sequence. *Colloids and Surfaces B: Biointerfaces*, 81(2), 452-460.
- 480 Asare-Addo, K., Levina, M., Rajabi-Siahboomi, A. R., & Nokhodchi, A. (2011). Effect of ionic
481 strength and pH of dissolution media on theophylline release from hypromellose matrix
482 tablets—Apparatus USP III, simulated fasted and fed conditions. *Carbohydrate*
483 *polymers*, 86(1), 85-93.
- 484 Asare-Addo, K., Kaialy, W., Levina, M., Rajabi-Siahboomi, A., Ghori, M. U., Supuk, E., ... &
485 Nokhodchi, A. (2013b). The influence of agitation sequence and ionic strength on in vitro drug
486 release from hypromellose (E4M and K4M) ER matrices—The use of the USP III
487 apparatus. *Colloids and Surfaces B: Biointerfaces*, 104, 54-60.
- 488 Asare-Addo, K., Conway, B. R., Larhrib, H., Levina, M., Rajabi-Siahboomi, A. R., Tetteh, J.,
489 ... & Nokhodchi, A. (2013a). The effect of pH and ionic strength of dissolution media on in-
490 vitro release of two model drugs of different solubilities from HPMC matrices. *Colloids and*
491 *Surfaces B: Biointerfaces*, 111, 384-391.
- 492 Bruschi, M. L. (2015). *Strategies to modify the drug release from pharmaceutical systems*.
493 Woodhead Publishing.
- 494 Charman, W. N., Porter, C. J., Mithani, S., & Dressman, J. B. (1997). Physicochemical and
495 physiological mechanisms for the effects of food on drug absorption: the role of lipids and
496 pH. *Journal of pharmaceutical sciences*, 86(3), 269-282.
- 497 Crowley, M. M., Zhang, F., Koleng, J. J., & McGinity, J. W. (2002). Stability of polyethylene
498 oxide in matrix tablets prepared by hot-melt extrusion. *Biomaterials*, 23(21), 4241-4248.

499 Ebube, N. K., Hikal, A. H., Wyandt, C. M., Beer, D. C., Miller, L. G., & Jones, A. B. (1997).
500 Sustained release of acetaminophen from heterogeneous matrix tablets: influence of polymer
501 ratio, polymer loading, and co-active on drug release. *Pharmaceutical development and*
502 *technology*, 2(2), 161-170.

503 Ford, J. L., Mitchell, K., Rowe, P., Armstrong, D. J., Elliott, P. N., Rostron, C., & Hogan, J. E.
504 (1991). Mathematical modelling of drug release from hydroxypropylmethylcellulose matrices:
505 effect of temperature. *International journal of pharmaceutics*, 71(1-2), 95-104.

506 Gao, F. (2004). Clay/polymer composites: the story. *Materials today*, 7(11), 50-55.

507 Gonçalves-Araújo, T., Rajabi-Siahboomi, A. R., & Caraballo, I. (2010). Polymer percolation
508 threshold in HPMC extended release formulation of carbamazepine and verapamil HCl. *Aaps*
509 *Pharmscitech*, 11(2), 558-562.

510 Kaialy, W., Bello, H., Asare-Addo, K., & Nokhodchi, A. (2016). Effect of solvent on retarding
511 the release of diltiazem HC I from Polyox-based liquisolid tablets. *Journal of Pharmacy and*
512 *Pharmacology*, 68(11), 1396-1402.

513 Hermann, P. H., Rodger, S. D., Remones, G., Thenot, J. P., London, D. R., & Morselli, P. L.
514 (1983). Pharmacokinetics of diltiazem after intravenous and oral administration. *European*
515 *journal of clinical pharmacology*, 24(3), 349-352.

516 Kanjanakawinkul, W., Rades, T., Puttipipatkachorn, S., & Pongjanyakul, T. (2013). Nicotine–
517 magnesium aluminum silicate microparticle surface modified with chitosan for mucosal
518 delivery. *Materials Science and Engineering: C*, 33(3), 1727-1736.

519 Khlibsuwan, R., & Pongjanyakul, T. (2016). Chitosan-clay matrix tablets for sustained-release
520 drug delivery: Effect of chitosan molecular weight and lubricant. *Journal of Drug Delivery*
521 *Science and Technology*, 35, 303-313.

522 Khlibsuwan, R., Siepmann, F., Siepmann, J., & Pongjanyakul, T. (2017). Chitosan-clay
523 nanocomposite microparticles for controlled drug delivery: Effects of the MAS content and
524 TPP crosslinking. *Journal of Drug Delivery Science and Technology*, 40, 1-10.

525 Khuathan, N., & Pongjanyakul, T. (2014). Modification of quaternary polymethacrylate films
526 using sodium alginate: film characterization and drug permeability. *International journal of*
527 *pharmaceutics*, 460(1-2), 63-72.

528 Kim, C. J. (1995). Drug release from compressed hydrophilic POLYOX-WSR tablets. *Journal*
529 *of Pharmaceutical Sciences*, 84(3), 303-306.

530 Klein S., Rudolph M.W., Dressman J.B. *Dissolution Technologies* (2002) (Article 1)

531 Li, J., Luo, C., Zhang, D., Li, M., Fu, Q., & He, Z. (2016). Formulation and development of
532 ternary hybrid matrix tablets of diltiazem hydrochloride. *Powder Technology*, 294, 66-70.

533 Lindahl, A., Ungell, A. L., Knutson, L., & Lennernäs, H. (1997). Characterization of fluids
534 from the stomach and proximal jejunum in men and women. *Pharmaceutical research*, 14(4),
535 497-502.

536 Ma, L., Deng, L., & Chen, J. (2014). Applications of poly (ethylene oxide) in controlled release
537 tablet systems: a review. *Drug development and industrial pharmacy*, 40(7), 845-851.

538 Maggi, L., Segale, L., Torre, M. L., Machiste, E. O., & Conte, U. (2002). Dissolution behaviour
539 of hydrophilic matrix tablets containing two different polyethylene oxides (PEOs) for the
540 controlled release of a water-soluble drug. Dimensionality study. *Biomaterials*, 23(4), 1113-
541 1119.

542 Mason, L. M., Campiñez, M. D., Pygall, S. R., Burley, J. C., Gupta, P., Storey, D. E., ... &
543 Melia, C. D. (2015). The influence of polymer content on early gel-layer formation in HPMC
544 matrices: the use of CLSM visualisation to identify the percolation threshold. *European*
545 *Journal of Pharmaceutics and Biopharmaceutics*, 94, 485-492.

546 Nep, E. I., Mahdi, M. H., Adebisi, A. O., Dawson, C., Walton, K., Bills, P. J., ... & Asare-
547 Addo, K. (2017). The influence of hydroalcoholic media on the performance of Grewia
548 polysaccharide in sustained release tablets. *International journal of pharmaceutics*, 532(1),
549 352-364.

550 Nokhodchi, A., Palmer, D., Asare-Addo, K., Levina, M., & Rajabi-Siahboomi, A. (2015).
551 Application of polymer combinations in extended release hydrophilic matrices. *Handbook of*
552 *Polymers for Pharmaceutical Technologies*, 1, 23-49.

553 Nokhodchi, A., Raja, S., Patel, P., & Asare-Addo, K. (2012). The role of oral controlled release
554 matrix tablets in drug delivery systems. *BioImpacts: BI*, 2(4), 175.

555 Okeke, O. C., & Boateng, J. S. (2017). Nicotine stabilization in composite sodium alginate
556 based wafers and films for nicotine replacement therapy. *Carbohydrate polymers*, 155, 78-88.

557 Okeke, O. C., & Boateng, J. S. (2016). Composite HPMC and sodium alginate based buccal
558 formulations for nicotine replacement therapy. *International journal of biological*
559 *macromolecules*, *91*, 31-44.

560 Ozeki, T., Yuasa, H., & Kanaya, Y. (1999). Control of medicine release from solid dispersion
561 composed of the poly (ethylene oxide)-carboxyvinylpolymer interpolymer complex by varying
562 molecular weight of poly (ethylene oxide). *Journal of controlled release*, *58*(1), 87-95.

563 Padial, L. R., Baron-Esquivias, G., Madrid, A. H., Martín, D. M., Pallares-Carratala, V., & de
564 la Sierra, A. (2016). Clinical experience with diltiazem in the treatment of cardiovascular
565 diseases. *Cardiology and therapy*, *5*(1), 75-82.

566 Palmer, D., Levina, M., Douroumis, D., Maniruzzaman, M., Morgan, D. J., Farrell, T. P., ... &
567 Nokhodchi, A. (2013). Mechanism of synergistic interactions and its influence on drug release
568 from extended release matrices manufactured using binary mixtures of polyethylene oxide and
569 sodium carboxymethylcellulose. *Colloids and Surfaces B: Biointerfaces*, *104*, 174-180.

570 Pappa, C., Nanaki, S., Giliopoulos, D., Triantafyllidis, K., Kostoglou, M., Avgeropoulos, A.,
571 & Bikiaris, D. (2018). Nanostructured Composites of Sodium Montmorillonite Clay and PEO
572 Used in Dissolution Improvement of Aprepitant Drug by Melt Mixing. *Applied Sciences*, *8*(5),
573 786.

574 Pongjanyakul, T., & Rojtanatanya, S. (2012). Use of propranolol-magnesium aluminium
575 silicate intercalated complexes as drug reservoirs in polymeric matrix tablets. *Indian journal*
576 *of pharmaceutical sciences*, *74*(4), 292.

577 Pongjanyakul, T., Khunawattanakul, W., Strachan, C. J., Gordon, K. C., Puttipipatkachorn,
578 S., & Rades, T. (2013). Characterization of chitosan–magnesium aluminum silicate
579 nanocomposite films for buccal delivery of nicotine. *International journal of biological*
580 *macromolecules*, *55*, 24-31.

581 Prasad, M. B., Vidyadhara, S., Sasidhar, R. L. C., Balakrishna, T., & Trilochani, P. (2013).
582 Development and evaluation of diltiazem hydrochloride controlled-release pellets by fluid bed
583 coating process. *Journal of advanced pharmaceutical technology & research*, *4*(2), 101.

584 Qazi, F., Shoaib, M. H., Yousuf, R. I., Qazi, T. M., Mehmood, Z. A., & Hasan, S. M. F. (2013).
585 Formulation development and evaluation of Diltiazem HCl sustained release matrix tablets
586 using HPMC K4M and K100M. *Pak J Pharm Sci*, *26*(4), 653-663.

587 Rongthong, T., Sungthongjeen, S., Siepmann, J., & Pongjanyakul, T. (2013). Quaternary
588 polymethacrylate–magnesium aluminum silicate films: molecular interactions, mechanical
589 properties and tackiness. *International journal of pharmaceutics*, 458(1), 57-64.

590 Rongthong, T., Sungthongjeen, S., Siepmann, F., Siepmann, J., & Pongjanyakul, T. (2020).
591 Eudragit RL-based film coatings: How to minimize sticking and adjust drug release using
592 MAS. *European Journal of Pharmaceutics and Biopharmaceutics*, 148, 126-133.

593 Rojtanatanya, S., & Pongjanyakul, T. (2010). Propranolol–magnesium aluminum silicate
594 complex dispersions and particles: Characterization and factors influencing drug
595 release. *International journal of pharmaceutics*, 383(1-2), 106-115.

596 Shojaee, S., Cumming, I., Kaialy, W., & Nokhodchi, A. (2013a). The influence of vitamin E
597 succinate on the stability of polyethylene oxide PEO controlled release matrix tablets. *Colloids
598 and Surfaces B: Biointerfaces*, 111, 486-492.

599 Shojaee, S., Asare-Addo, K., Kaialy, W., Nokhodchi, A., & Cumming, I. (2013b). An
600 investigation into the stabilization of diltiazem HCl release from matrices made from aged
601 polyox powders. *AAPS PharmSciTech*, 14(3), 1190-1198.

602 Shojaee, S., Nokhodchi, A., Cumming, I., Alhalaweh, A., & Kaialy, W. (2015). Investigation
603 of drug release from PEO tablet matrices in the presence of vitamin E as antioxidant. *Current
604 drug delivery*, 12(5), 591-599.

605 Siahi-Shadbad, M. R., Asare-Addo, K., Azizian, K., Hassanzadeh, D., & Nokhodchi, A.
606 (2011). Release behaviour of propranolol HCl from hydrophilic matrix tablets containing
607 psyllium powder in combination with hydrophilic polymers. *Aaps Pharmscitech*, 12(4), 1176-
608 1182.

609 Siepmann, J., & Peppas, N. A. (2001). Mathematical modeling of controlled drug
610 delivery. *Advanced drug delivery reviews*, 48(2-3).

611 Siepmann, J., & Peppas, N. A. A. (2012). Modeling of drug release from delivery systems
612 based on hydroxypropyl methylcellulose (HPMC). *Advanced drug delivery reviews*, 64, 163-
613 174.

614 Totea, A. M., Dorin, I., Gavrilov, G., Laity, P. R., Conway, B. R., Waters, L., & Asare-Addo,
615 K. (2019). Real time calorimetric characterisation of clay–drug complex dispersions and
616 particles. *International journal of pharmaceutics: X*, 1, 100003.

617 Totea, A. M., Sabin, J., Dorin, I., Hemming, K., Laity, P. R., Conway, B. R., ... & Asare-Addo,
618 K. (2020). Thermodynamics of clay–drug complex dispersions: Isothermal titration
619 calorimetry and high-performance liquid chromatography. *Journal of Pharmaceutical*
620 *Analysis*, 10(1), 78-85.

621 Ward, A., Walton, K., Mawla, N., Kaialy, W., Liu, L., Timmins, P., ... & Asare-Addo, K.
622 (2019). Development of a novel method utilising dissolution imaging for the measurement of
623 swelling behaviour in hydrophilic matrices. *International journal of pharmaceutics: X*, 1,
624 100013.

625 Ward, A., Walton, K., Stoycheva, S., Wallis, M., Adebisi, A., Nep, E., ... & Asare-Addo, K.
626 (2020). The use of visible and UV dissolution imaging for the assessment of propranolol
627 hydrochloride in liquisolid compacts of *Sesamum radiatum* gum. *Journal of Drug Delivery*
628 *Science and Technology*, 101511.

629 Washington, N., Washington, C., & Wilson, C. (2000). *Physiological pharmaceutics: barriers*
630 *to drug absorption*. CRC Press.

631 Vanderbilt Minerals (2014a) *VEEGUM / VAN GEL Magnesium Aluminum Silicate Magnesium*
632 *Aluminum Silicate ® The Story*. Norwalk.

633 Vanderbilt Minerals (2014b) ‘VEEGUM ® Magnesium Aluminum Silicate VANATURAL ®
634 Bentonite Clay For Personal Care and Pharmaceuticals What They Are’, pp. 1–27.

635 Velasco, M. V., Ford, J. L., Rowe, P., & Rajabi-Siahboomi, A. R. (1999). Influence of drug:
636 hydroxypropylmethylcellulose ratio, drug and polymer particle size and compression force on
637 the release of diclofenac sodium from HPMC tablets. *Journal of Controlled Release*, 57(1), 75-
638 85.

639

640